Advanced Composite Materials
Publication details, including instructions for authors and subscription information:
http://www.tandfonline.com/loi/tacm20

Bonding and debonding behavior of FRP sheets under fatigue loading

Kentaro Iwashita [a], Zhishen Wu [b], Takashi Ishikawa [c], Yasumasa Hamaguchi [d] & Toshio Suzuki [e]

[a] Department of Urban and Civil Engineering, Ibaraki University, Nakanarusawa-cho 4-12-1, Hitachi-shi, Ibaraki-ken 316-8511, Japan

[b] Department of Urban and Civil Engineering, Ibaraki University, Nakanarusawa-cho 4-12-1, Hitachi-shi, Ibaraki-ken 316-8511, Japan

[c] Advanced Composite Evaluation Technology Center (ACE TeC), Institute of Space Technology and Aeronautics, Japan Aerospace Exploration Agency (JAXA), 6-13-1, Ohsawa, Mitaka, Tokyo 181-0015, Japan

[d] Advanced Composite Evaluation Technology Center (ACE TeC), Institute of Space Technology and Aeronautics, Japan Aerospace Exploration Agency (JAXA), 6-13-1, Ohsawa, Mitaka, Tokyo 181-0015, Japan

[e] Department of Urban and Civil Engineering, Ibaraki University, Nakanarusawa-cho 4-12-1, Hitachi-shi, Ibaraki-ken 316-8511, Japan

Version of record first published: 02 Apr 2012.

To cite this article: Kentaro Iwashita , Zhishen Wu , Takashi Ishikawa , Yasumasa Hamaguchi & Toshio Suzuki (2007): Bonding and debonding behavior of FRP sheets under fatigue loading, Advanced Composite Materials, 16:1, 31-44

To link to this article: http://dx.doi.org/10.1163/156855107779755291

Adv. Composite Mater., Vol. 16, No. 1, pp. 31–44 (2007)

Also available online - www.brill.nl/acm

Bonding and debonding behavior of FRP sheets under fatigue loading

KENTARO IWASHITA [1], ZHISHEN WU [1], TAKASHI ISHIKAWA [2], YASUMASA HAMAGUCHI [2] and TOSHIO SUZUKI [1]

[1] *Department of Urban and Civil Engineering, Ibaraki University, Nakanarusawa-cho 4-12-1, Hitachi-shi, Ibaraki-ken 316-8511, Japan*
[2] *Advanced Composite Evaluation Technology Center (ACE TeC), Institute of Space Technology and Aeronautics, Japan Aerospace Exploration Agency (JAXA), 6-13-1, Ohsawa, Mitaka, Tokyo 181-0015, Japan*

Received 19 December 2005; accepted 24 February 2006

Abstract—The purpose of this study is to improve the examining and understanding of the bonding behavior of Fiber Reinforced Polymer (FRP) sheets bonded to concrete blocks and steel plates under fatigue loading. First, a series of experimental investigations is summarized in the paper. The fatigue behavior of bonding surface between FRP sheets and concrete is finally characterized by the conducted P–S–N diagram representing the relationship among the probability of FRP debonding (P), the bond stress amplitudes (S), and the number of cycles (N) at debonding on a semi-logarithmic scale. The different debonding modes for various fracturing surface are also investigated and evaluated.

Keywords: FRP sheets; concrete; steel plate; bond; fatigue; shear test; P–S–N curve.

1. INTRODUCTION

The need to rehabilitate or upgrade deteriorating civil infrastructure is becoming a major and urgent problem worldwide. In contrast with the traditional strengthening methods, such as overlaying and jacketing method, external cable method and bonded and jacketing steel plate method, the use of fiber reinforced polymers (FRP) represents an innovative and effective technology for strengthening of infrastructure. In recent years, repairing and strengthening concrete structures with externally applied, epoxy-bonded FRP sheets to the tension face of structural element has been

Edited by the JSCM.
E-mails: iwak@mx.ibaraki.ac.jp; zswu@mx.ibaraki.ac.jp; isikawa@chofu.jaxa.jp; hamaguchi.yasumasa@jaxa.jp

widely accepted for practical uses. On the other hand, recent studies have also reported a variety of FRP debonding problems. Although the bonding and debonding mechanisms of FRP sheets under static loading have been quite extensively studied, until now, the study of FRP bonding and debonding behavior under fatigue loading, especially for the case of the fundamental mechanism of FRP fracture behavior, has rarely been carried out. For strengthening traffic structures, the evaluation of fatigue performances is considered to be a very important one. Based on these considerations, this paper aims at investigating clearly the bonding behavior of FRP sheets bonded to concrete and steel structures under fatigue loading. First, a summary of a series of experimental investigations is given. The fatigue behavior of FRP bonding is finally characterized by the conducted S–N diagram representing the relationship between the bond stress amplitudes (S) and the number of cycles (N) to debonding on a semi-logarithmic scale. Thereafter, relationships between debonding modes and bond capacity under fatigue loading are evaluated from the debonding probability (P)–S–N curve which is recommended by the JSCM standard evaluation method [1]. In this study, a newly developed PBO (poly-*p*-phenylene-benzobisoxazole) fiber sheet, which has been accepted as reinforcement, is used.

2. SPECIMENS

2.1. Specimens of FRP sheets–concrete double-lap bonding joints

In accordance with the experimental method of JSCE Recommendations for Upgrading of Concrete Structures with Use of Continuous Fiber Sheets [2], prism specimens whose size is 100 mm width, 100 mm thick and 600 mm long are used in the investigation. The specimen is cut off at the position of the notch (pre-crack). The details of the prism specimens are schematically shown in Fig. 1. Before bonding of FRP sheet, the concrete surface preparation is treated with a diamond sander, and an epoxy primer is painted after wiping with cloth soaked with acetone. One layer FRP sheet whose size is 50 mm width and 400 mm span is impregnated with epoxy resin before it is bonded to the concrete surface, and bonded to both sides of the concrete block along the axial direction after hardening of adhesive by the end of 24 h. Moreover, the tensile test is started 7 days after and is followed by the bonding of FRP sheets. The tensile load is applied by pulling both ends of the steel plate. A summary of the properties of PBO fiber sheets, the epoxy resin and the concrete is shown in Table 1.

2.2. Specimens of FRP sheets–steel plate single-lap bonding joints

In accordance with the experimental method of JSCE Recommendations [2], the single-lap shear specimens of dimensions 400 mm long, 1.6 mm thick and 12.5 mm width are used in the investigation. The details of the shear specimens are

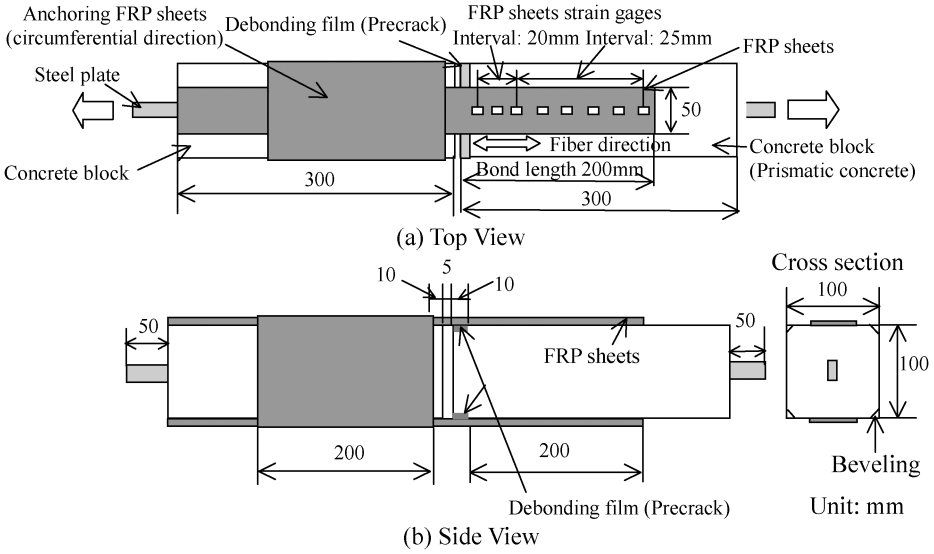

Figure 1. Specimen dimensions of FRP sheets–concrete bonding joints.

Table 1.
Summary of material properties

Concrete	Compressive strength (MPa)	36.8
	Modulus of elasticity (GPa)	30.0
	Poisson's ratio	0.3
PBO fiber reinforced polyer sheets	Guaranteed tensile strength (MPa)	3500
	Guaranteed modulus of elasticity (GPa)	235
	Nominal thickness (mm)	0.128
Steel plate (SM490)	Guaranteed tensile strength (MPa)	490
	Guaranteed yielding stress (MPa)	325
	Guaranteed modulus of elasticity (GPa)	210
Epoxy resin (FR-E3P)	Guaranteed tensile strength (MPa)	51.9
	Guaranteed tensile shear strength (MPa)	25
	Guaranteed modulus of elasticity (GPa)	3.43

schematically shown in Fig. 2. FRP sheets are bonded to one side of the steel plate along the axial direction. A tensile load is applied by pulling each ends of the steel plate and FRP sheets. Before bonding of FRP sheet, the concrete surface preparation is treated with the No.100 sand paper and wiped with a cloth soaked with acetone. Details of the steel plate are shown in Table 1.

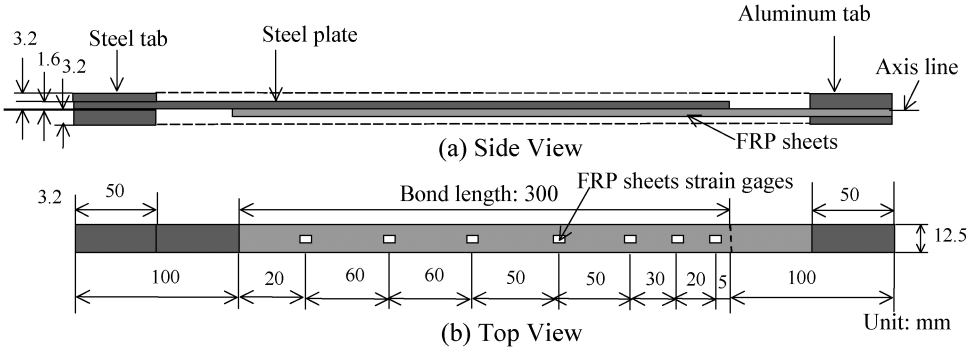

Figure 2. Specimen dimensions of FRP sheets–steel plate bonding joints.

3. EXPERIMENTAL PROGRAM

3.1. Experimental program of FRP sheets–concrete double-lap bonding joints

In this investigation, an Instron 8502 series fatigue testing machine and the 100 kN load cell are used to measure the load acting on the specimen and the position of lower grip. The arrangement of wire strain gages whose effective longitude is 5 mm to measure FRP strains is shown in Fig. 1. The repetition frequency of cyclic loading is 5 Hz. The variables of maximum repeated loads are set as 20%, 30%, 40%, 50%, 60% and 70% of static load of FRP sheet f_u, which is identified as minimum value among the load carrying capacities investigated by the three static tests, and the minimum repeated load is set as 10% of f_u in all experiments. Table 2 summarizes the results of specimens of FRP-concrete bonding joints. If the FRP debonding has not occurred after 2 million cycles of loading, the static loading test is carried out with a loading rate of 1 kN/min. The test temperature is about 24–27°C.

3.2. Experimental program of FRP sheets–steel plate single-lap bonding joints

In this investigation, an Instron 8502 series fatigue testing machine and the 100 kN load cell are used to measure the load acting on the specimen and the position of the lower grip. The arrangement of wire strain gages whose effective longitude is 5 mm to measure FRP strains is shown in Fig. 2. The repetition frequency of cyclic loading is about 4 Hz. The test specimens are summarized as shown in Table 3. The variables of maximum repeated load ratios are selected as 16.5%, 33.1%, 44.1%, 55.1%, 66.1%, 71.6% and 77.1% of f'_u, which is the identified minimum value among the load carrying capacities investigated by the three static tests, and the minimum load ratio is set as 11.0% of f'_u in all experiments. If the FRP debonding has not occurred after 2 million cycles of loading, then a static loading test is carried out with a loading rate of 1 kN/min. The test temperature is about 25–27°C.

Table 2.
Summary of FRP sheets–concrete bonding tests

Specimens	Maximum load ratio* (%)	Maximum load P_{cmax}* (kN)	Minimum load ratio* (%)	Minimum load P_{cmin}* (kN)	Number of specimens
CS-1,2,3	**	**	**	**	3
CF-70-1,2,3	70	19.6	10	2.8	3
CF-60-1,2,3	60	16.8	10	2.8	3
CF-50-1,2,3	50	14.0	10	2.8	3
CF-40-1,2,3	40	11.2	10	2.8	3
CF-30-1,2	30	8.4	10	2.8	2
CF-20-1,2	20	5.6	10	2.8	2

* The value of minimum static debonding load P_{cu} is 28 kN.
** Under static loading.

Table 3.
Summary of FRP sheets–steel plate bonding tests

Specimens	Maximum load ratio* (%)	Maximum load P_{smax}* (kN)	Minimum load ratio* (%)	Minimum load P_{smin}* (kN)	Number of specimens
SS-1,2,3	**	**	**	**	3
SF-77.1-1,2,3	77.1	4.550	11.0	0.65	3
SF-71.6-1,2,3	71.6	4.225	11.0	0.65	3
SF-66.1-1,2,3,4,5	66.1	3.900	11.0	0.65	5
SF-55.1-1,2	55.1	3.250	11.0	0.65	2
SF-44.1-1,2,3	44.1	2.600	11.0	0.65	3
SF-33.1-1,2,3	33.1	1.950	11.0	0.65	3
SF-16.5-1,2,3	16.5	0.975	11.0	0.65	3

* The value of minimum static debonding load P_{su} is 5.9 kN.
** Under static loading.

4. EXPERIMENTAL RESULTS AND DISCUSSION

4.1. Experimental results of FRP sheets–concrete double-lap bonding joints

The load–displacement curves for different static tests of FRP-concrete joint under static loading are shown in Fig. 3, in which the specimen CF-20-1 is subjected to static load after 2 million cycles of loading. Micro-debonding initiates at the tensile end of bonded FRP sheets, and propagates gradually to form a macro-debonding. Once the macro-debonding length grows to about 20–30 mm, debonding propagates towards the free end of bonded FRP sheet. Finally, a complete FRP sheet debonding occurs when debonding propagation reaches a critical value. The maximum loads and debonding modes are summarized in Table 4. In these experiments, three kinds of debonding modes due to different concrete surfaces conditions are observed as shown in Fig. 4. It is found that the load-carrying capacities for different debonding modes are different. The debonding mode B has a debonding into cement mortar, and debonding mode A has a debonding at the interface between epoxy resin and

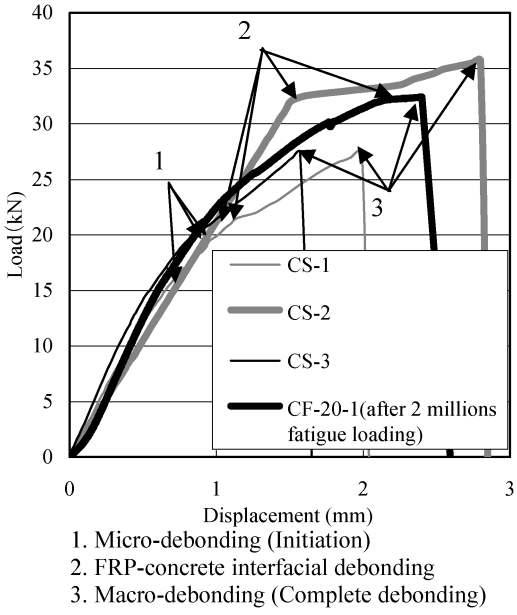

Figure 3. Load–displacement for static test.

Table 4.
Summary of FRP sheets–concrete bonding test under static loading

Specimen	Maximum load P_{cmax} (kN)	Debonding mode	Effective bond length L_{ce} (mm)	Bond stress τ_{cu} (MPa)	Interfacial fracture energy G_{cf} (MPa mm)
CS-1	27.5	A	130	2.12	1.26
CS-2	35.3	A^+	125	2.82	2.12
CS-3	27.5	B	95	2.89	1.28
CF-20-1	32.5	A^+	120	2.71	1.75
CF-70-1	*	B	80	*	*
CF-70-2	*	B	80	*	*
CF-70-3	*	A^+	115	*	*
CF-60-1	*	A^+	120	*	*
CF-60-2	*	A^+	80	*	*

* Under fatigue loading.

epoxy primer, while debonding mode A^+ has some debonding into coarse aggregate but it is similar to the case A. The load-carrying capacity with debonding mode A^+ is larger than ones with debonding modes A and B. The results of prism tests are investigated for the determination of interfacial fracture energy (G_{cf}) and bond strength (τ_{cu}). G_{cf} and τ_{cu} are calculated from equation (1) and equation (2),

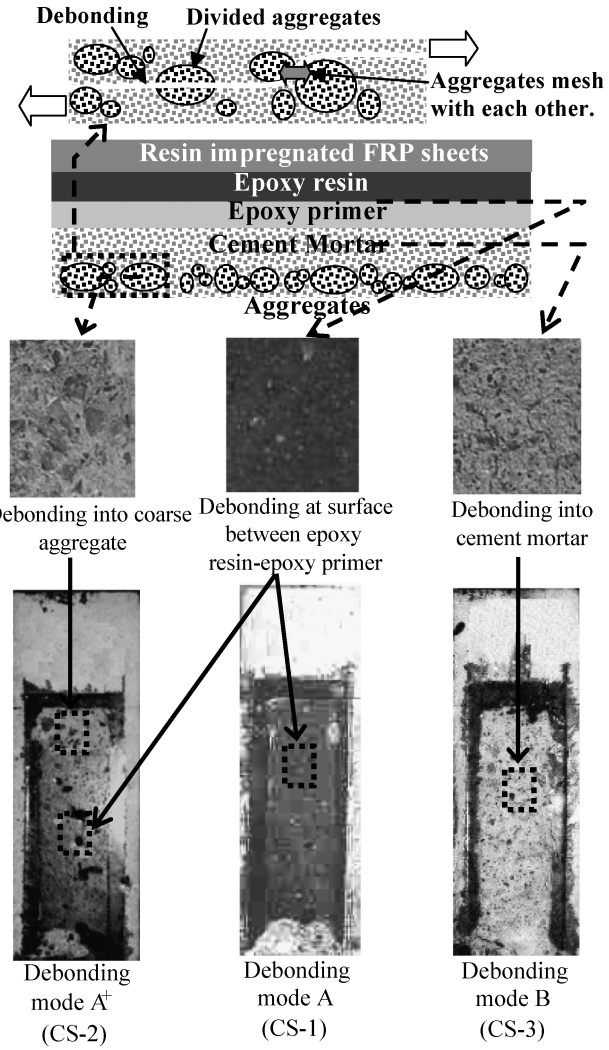

Figure 4. Debonding modes FRP sheets–concrete interface.

respectively:

$$G_{cf} = \frac{P_{\max}^2}{8b^2 E_{\mathrm{f}} t}, \tag{1}$$

$$\tau_{cu} = \frac{P_{\max}}{2bL_{\mathrm{e}}}, \tag{2}$$

where P is the maximum transferable force in FRP sheet; E_{f}, b and t are modulus of elasticity, width and thickness of FRP sheets respectively. Effective bonding length (L_{e}) is defined as the distance from the pre-crack of prism specimen to the position where 97% strain of the value at the pre-crack occurs [3]. These L_{e} values

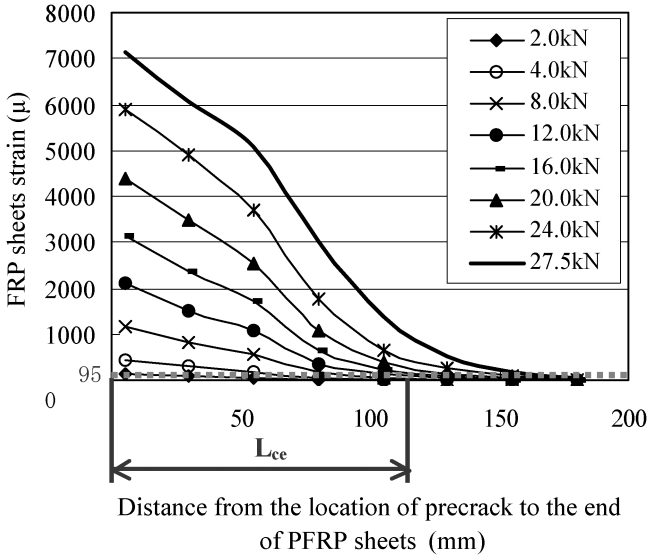

Figure 5. FRP sheets strain distribution of FRP sheets–concrete bonding test (CS-1).

of all specimens are about 100 mm. From Table 4, it is seen that the values of τ_{cu} with mode A^+ and B specimens are larger than that with mode A specimens. Moreover, the values of G_{cf} of mode A^+ specimens are larger than that of mode A and B specimens. Figure 5 shows the FRP strain distribution along the fiber direction of the CS-3 under different static loading stages. On the other hand, Fig. 6 shows the FRP strain distribution along the fiber direction of the CF-60-2 during the cyclic loading. Then, the FRP strain at the initiation of debonding during cyclic loading is considerably smaller than the case of static loading. During the experiments, it is found that the debonding fracture propagated gradually from the initiation to the FRP end for the case of static loading test. However, the debonding propagation after the initiation of debonding for the case of fatigue loading became brittle comparing with the case of static loading. Table 5 summarizes the results of fatigue test, and Fig. 7 shows the S–N curve with a semi-logarithmic scale. The results show that the upper limit of the maximum load ratio is about 20–30% when the debonding has not occurred after 2 million cycles of loading.

In accordance with the JSMS Standard Evaluation Method [1], the probability density distribution of all data is provided. In this method, it is considered that the distribution of all data along the maximum stress axis is similar to the standard normal distribution. The equation of the standard normal distribution is

$$\Phi(z) = \int_{-\infty}^{z} \frac{1}{\sqrt{2\pi}} \mathrm{e}^{u^2/2}\,\mathrm{d}u \quad (-\infty < z < \infty). \tag{3}$$

Moreover, maximum stress ratio x is calculated by the relationship among destruction probability $P(z)$, debonding probability μ and standard deviation σ as shown

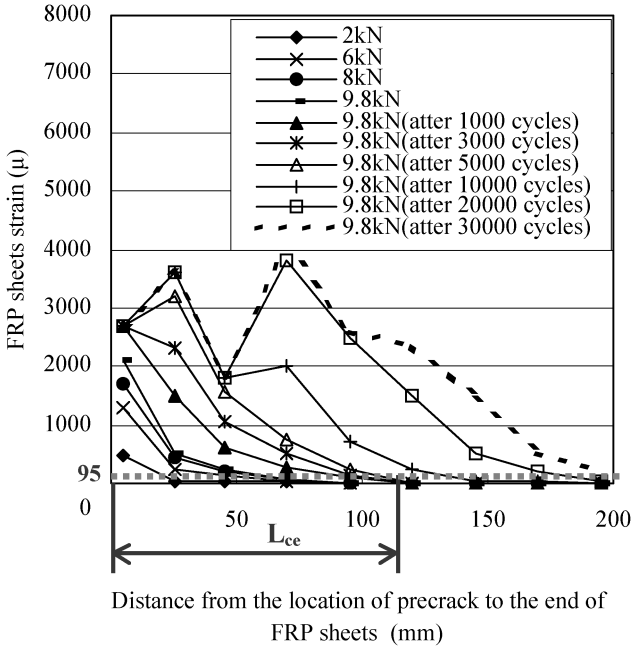

Figure 6. FRP sheets strain distribution of FRP sheets–concrete bonding test (CF-60-2).

Table 5.
Summary of fatigue tests of FRP sheets–concrete bonding joints

Specimen	Number of cycles	Debonding mode
CF-70-1	696	B
CF-70-2	2,808	B
CF-70-3	12,997	A^+
CF-60-1	30,593	A^+
CF-60-2	37,700	A^+
CF-60-3	25,136	B^+
CF-50-1	37,141	A
CF-50-2	17,986	B
CF-50-3	15,887	A
CF-40-1	206,728	A
CF-40-2	203,077	A
CF-40-3	343,223	A^+
CF-30-1	1,986,573	A^+
CF-30-2	2,000,000	No failure
CF-20-1	2,000,000	No failure
CF-20-2	2,000,000	No failure

in equation (4):

$$x = \Phi\big(1 - P(z)\big)\sigma + \mu. \tag{4}$$

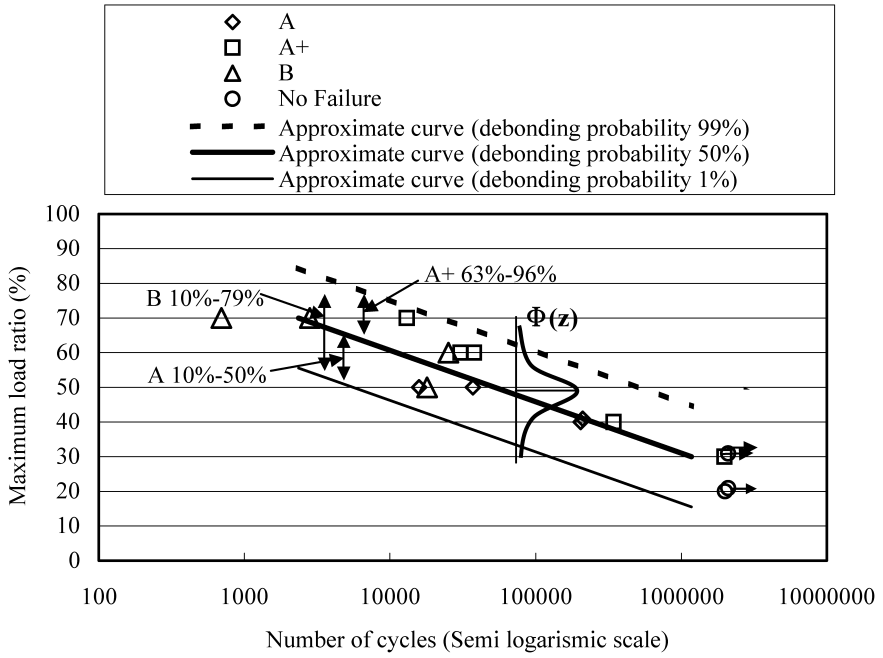

Figure 7. P–S–N curve for FRP sheets–concrete bonding tests.

As an example, S–N curves, considering the debonding probabilities equal to 1% and 99%, are shown in Fig. 7. Then, most of the data are distributed near the 50% S–N curve, so the higher reproduction characteristic of this experiment is proved. On the other hand, debonding probabilities of the specimens whose debonding mode is A^{+}(63–96%) are higher than that of the specimens whose debonding mode is A (10–50%) and B (10–79%). In addition, tensile strengths of cement mortar, fine aggregate and an epoxy primer are about 3 MPa and lower than that of a rough aggregate (about 20 MPa).

4.2. Experimental results of FRP sheets–steel plate with single-lap bonding joints

The load–displacement curves for the steel plate-FRP single-lap shear tests areas shown in Fig. 8, in which the specimen SF-18.4-1 is subjected to static loading after the fatigue loading of 2 million cycles. Micro-debonding initiates at the tensile end of bonded FRP sheets, and propagates gradually to form a macro-debonding. Once macro-debonding length grows to about 20–30 mm, debonding propagates towards the free end of bonded FRP sheet. Finally, a complete FRP sheet debonding occurs when debonding propagation reaches a critical value. Table 6 shows the summary of experimental results for both maximum loads and debonding modes. The debonding modes can be divided into three patterns due to the steel plate surface condition after FRP debonding, and shown in Fig. 9. The debonding mode A has a debonding fracture within the FRP layer, and the debonding mode B has a debonding fracture within the inside of the epoxy resin, while the debonding mode C has a fracture

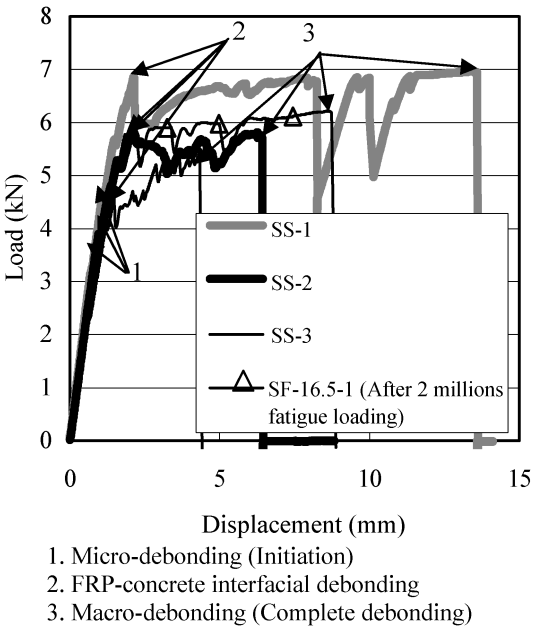

Figure 8. Load–displacement curves for steel plate-FRP sheets bonding tests under static loading.

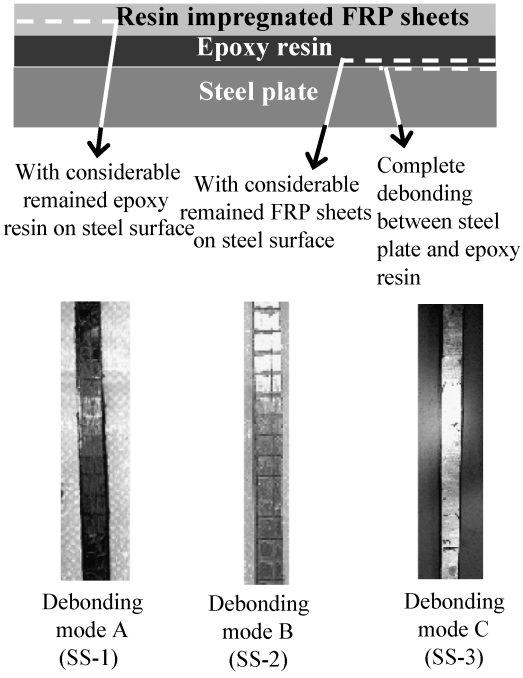

Figure 9. Debonding modes of steel plate-FRP sheets bonding joints.

Table 6.
Summary of FRP sheets–steel plate bonding test under static loading

Specimens	Maximum load P_{smax} (kN)	Debonding mode	Effective bond length L_{se} (mm)	Bond stress τ_{su} (MPa)	Interfacial fracture energy G_{sf} (MPa mm)
SS-1	6.97	A	110	5.07	5.17
SS-2	5.88	B	110*	4.28	3.68
SS-3	6.13	C	110*	4.46	4.00
SF-16.5-1	6.18	C	110*	4.49	4.06
SF-16.5-2	6.22	B	110*	4.52	4.12

* The effective bond length of SS-2∼SF16. 5-2 is assumed 110 mm from the SS-1 measurement.

between epoxy resin and steel plate interface. The load carrying capacity due to the debonding mode A is larger than the ones due to other debonding modes B and C. Moreover, both debonding modes B and C have similar performance on debonding loading. The experimental results are investigated for the determination of interfacial fracture energy (G_{sf}), bond strength (τ_{su}). G_{sf} and τ_{su} are calculated from equation (5) and equation (6), respectively:

$$G_{sf} = \frac{\mathrm{P}_{\text{max}}^2}{8b^2 E_{\text{f}} t}, \tag{5}$$

$$\tau_{su} = \frac{P_{\text{max}}}{2bL_{\text{e}}}, \tag{6}$$

where P is the maximum load; E_{f}, b and t are modulus of elasticity, width and thickness of FRP sheets, respectively. The values of τ_{su} of mode A specimens are larger than that of mode B and C specimens as may be seen from Table 6. Table 7 summarizes the results of fatigue test, and Fig. 10 shows the conducted S–N curve of steel plate-FRP tests under fatigue loading. The results show that the upper limit of the maximum load ratio is about 18–30% when the debonding has not occurred after 2 million loading cycles.

As an example, S–N curves, considering the debonding probabilities equal 1% and 99%, are shown in Fig. 10. Then, most of the data are distributed near the 50% S–N curve, which verifies the higher reproduction characteristics of this experiment. On the other hand, debonding probabilities of the specimens whose debonding mode is C (44–84%) are higher than that of the specimens whose debonding mode is B (7–77%).

5. CONCLUSIONS

From the study carried out, different debonding modes of FRP sheets, bonded on concrete and steel surfaces, are observed. The load carrying capacity for different debonding modes, the interfacial fracture energy and the bond strength are evaluated

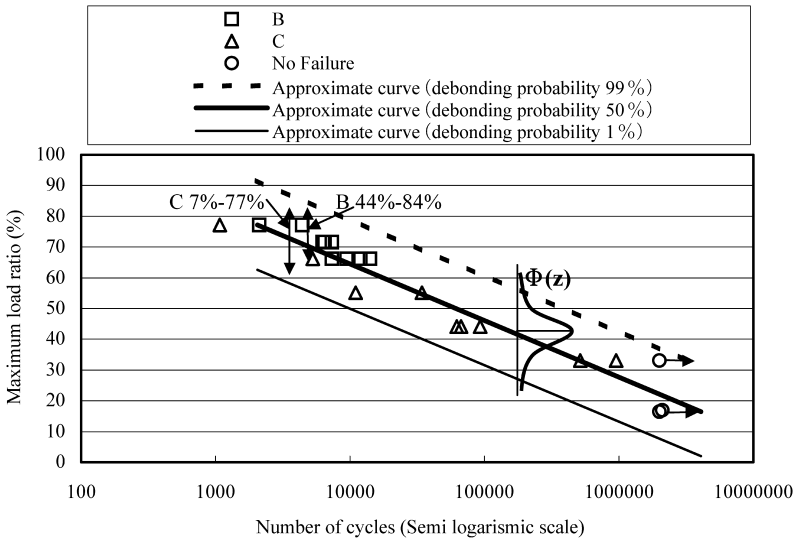

Figure 10. P–S–N curve for FRP sheets–steel plate bonding test.

Table 7.
Summary of fatigue tests of FRP sheets–steel plate bonding joints

Specimens	Number of cycles	Debonding mode
SF-77.1-1	4,412	B
SF-77.1-2	1,078	C
SF-77.1-3	2,114	B
SF-71.6-1	6,255	B
SF-71.6-2	7,324	B
SF-71.6-3	6,480	B
SF-66.1-1	14,058	B
SF-66.1-2	9,458	B
SF-66.1-3	11,985	B
SF-66.1-4	5,288	C
SF-66.1-5	7,306	B
SF-55.1-1	34,362	C
SF-55.1-2	11,015	C
SF-44.1-1	93,199	C
SF-44.1-2	67,089	C
SF-44.1-3	62,411	C
SF-33.1-1	515,619	C
SF-33.1-2	2,000,000	C
SF-33.1-3	2,000,000	C
SF-16.5-1	2,000,000	C
SF-16.5-2	2,000,000	C
SF-16.5-3	2,000,000	C

for static and cyclic loading as well. Based on the results of this experimental study, the following conclusions are drawn:

(1) Interfacial fracture energies from the static tests and debonding probabilities from the fatigue tests of the specimens whose debonding mode are A^+ are higher than that of the specimens whose debonding modes are A and B. Higher aggregate shear strength than that of cement mortar is considered as the reason for showing the higher values of interfacial fracture energy and debonding probability with debonding mode A^+. This result indicates the necessity of removing the cement mortar from the concrete surface before the FRP sheets are bonded.

(2) Interfacial fracture energies from the static tests of the specimens whose debonding mode are A are higher than that of the specimens whose debonding mode are B and C. Therefore, debonding probabilities from the fatigue tests of the specimens whose debonding mode are B are higher than that of the specimens whose debonding mode are C. However, more experimental data are required to establish the relationship.

(3) The upper limit of the maximum load ratio is about 20–30% when the debonding is not occurred after 2 million loading cycles. Moreover, based on the limited data, the value for FRP-steel plate bonding specimens is predicted as 18–30%.

(4) During cyclic loading, the FRP strains at the initiation of debonding are considerably smaller than the case of static loading. In the fatigue testing, effective bond length increases gradually, and finally, FRP debonding occurs.

Acknowledgement

The authors would like to thank all the members of the P-PUT R&D consortium for their useful advices.

REFERENCES

1. Standard Evaluation Method of Fatigue Reliability for Metallic Materials – Standard Regression Method of S-N Curves – JSMS-SD-6-02, JSMS Committees on Fatigue and Reliability Engineering (2002).
2. Recommendations for Upgrading of Concrete Structures with Use of Continuous Fiber Sheets, Concrete Engineering Series 41, JSCE (2001).
3. H. Yoshizawa, Z. S. Wu, H. Yuan and T. Kanakubo, Study on FRP-concrete interface bond performance, *J. Mater. Concrete Struct. Pavement*, JSCE **662**, 105–119 (2000).
4. Z. S. Wu, K. Iwashita, T. Ishikawa and Y. Hamaguchi, Bonding and debonding behavior of FRP sheets under fatigue loading, in: *Proc. 10th US–Japan Confer. Compos. Mater.*, Standford, CA, pp. 810–818 (2002).